

A case of time-dependent anisotropy of low-field susceptibility (AMS)

Graham J. Borradaile*, Ieva Geneviciene

Department of Geology and Physics, Lakehead University, Thunder Bay, Ontario P7B 5E1, Canada

Received 1 November 2006; received in revised form 29 March 2007; accepted 12 April 2007

Abstract

A suite of non-tectonized, Meso-Proterozoic siliceous crystal tuffs and volcanic breccia with a visible stratification has a modal bulk susceptibility (k) $\sim 160 \mu\text{SI}$ [mean; S.D. = $141 \mu\text{SI}$; $44 \mu\text{SI}$]. Normally, such susceptibilities suffice to make reliable measurements of anisotropy of low field susceptibility (AMS) using AC induction-coil instruments. However, for this suite, time-dependent susceptibility – variations during measurement are large in comparison to susceptibility – differences along different axes through a specimen. Thus, in many specimens, AMS axes determined by routine induction coil measurement in a (Sapphire Instruments SI2B; 19,200 Hz, 60 A/m) measurement procedures are not reproducible. The apparent variation of specimen susceptibility during a single, four minute AMS measurement can $> 2 \mu\text{SI}$ whereas in the same interval the noise-level of our instrument is $< 0.2 \mu\text{SI}$. Thus, the time-dependence of the specimen-susceptibility is an intrinsic phenomenon due to the characteristics (grain size, domain structure) of the magnetite which dominates susceptibility during measurement and handling. Two procedures improved the reproducibility and stability of AMS axial orientations in some specimens. First, for some specimens, one or two cycles of LTD or AF demagnetization ($\leq 15 \text{ mT}$) stabilized AMS axes. (Previous workers have observed that LTD and AF demagnetization may change slightly the AMS of polydomainal magnetite). Of course, exposure to alternating fields is preferably avoided before any AMS study. Second, for some specimens AMS measurement were improved by shielding the induction coil instrument in a large magnetically shielded space (ambient field $< 5 \text{ nT}$). Further improvements were achieved by permitting the specimens to relax in side a magnetic shield for 24 h before measurement. The occurrence of time-dependent bulk susceptibility, especially noticeable in its AMS axial orientations is certainly a rare phenomenon and the procedures we used to improve measurement are excessive and unnecessary safeguards in routine AMS work; in any case, they mostly failed to produce a desirable degree of reproducibility. However, a simple test to detect for the presence of such time-dependent AMS is to repeat measurements at intervals of several hours, between which the specimen is permitted to relax in different orientations with respect to the geomagnetic field, or in a shielded space.

© 2007 Published by Elsevier B.V.

Keywords: Time-dependent susceptibility; AC susceptibility; Low field susceptibility; Anisotropy of magnetic susceptibility; AMS; Magnetic fabric; Volcanic flow fabric; Viscous magnetism

1. Goals and introduction

The petrofabric or orientation–distribution of certain minerals in rocks is commonly related to some pattern of

flow, due to strain in tectonically deformed rock, plastic flow in plutonic and metamorphic rock, or viscous flow in magma or sediments. Orientation distribution was notoriously difficult to quantify directly, either from grain-shape or the orientation of crystallographic axes. Sample preparation was laborious and commonly less than 100 measurements would be obtained from a single

* Corresponding author. Tel.: +1 807 683 0680.

E-mail address: borradaile@lakeheadu.ca (G.J. Borradaile).

specimen. Ising (1942a,b) and Graham (1954) recognized that “magnetic fabric” (the anisotropy of the specimen’s susceptibility in a low field, or AMS) was commonly a good proxy for the orientation–distribution (\sim petrofabric) of most high susceptibility minerals in the rock. Induced magnetization must be measured in a low field, similar to the geomagnetic field (say, ~ 80 A/m) so that remanence-bearing minerals respond linearly (without hysteresis) to the applied field. We now understand that the direct equivalence of magnetic fabric with petrofabric is complicated by many factors, most importantly the fact that multiple minerals with different orientation distributions and different anisotropies contribute to the measured AMS (Borradaile and Jackson, 2004). The relative importance of each mineral species depends on their relative abundance, the similarity of their orientation–distributions and on their mean susceptibility. Poorly abundant remanence-bearing minerals (RBM) may control the AMS since their bulk (mean) susceptibility is large (e.g., magnetite 2.2 SI, hematite ≤ 0.04 SI) compared to rock-forming minerals (mafic silicates $\ll 0.002$ SI, felsic silicates $\sim -14 \times 10^{-6}$ SI). Magnetite is usually an accessory ($<1\%$ volume) mineral and in the rocks studied here its abundance rarely exceeds 2000 ppm but hematite is abundant and visual inspection alone would suggest that the AMS of these felsic rocks is a function of magnetite and hematite concentrations and preferred orientations. We ascertained the mineralogical controls on susceptibility may be determined from magnetic tests on rocks and mineral separations. Also, orientations analysis may alert one to heterogeneous controls on magnetic fabric. These include comparisons of AMS orientations for groups of specimens with different bulk susceptibility and comparisons of the orientation of the mean tensor for a sample of specimens with the specimens normalized and then not normalized by their mean susceptibility.

If AMS is controlled entirely by rock-forming silicates or by carbonates, its association with the petrofabric elements is relatively simple. This is because most silicates are paramagnetic ($0 < k \leq 2000 \mu\text{SI}$) having a positive constant susceptibility that relates the measuring field (H) to the induced magnetization (M) according to $M = kH$. In the rare case where diamagnetic minerals such as quartz, feldspars and calcite are pure, $M = kH$ and $k \sim -14 \mu\text{SI}$. However, for rock dominated by diamagnetic rock-forming minerals (e.g., calcite, quartz, feldspar), trace concentrations of RBM, especially magnetite impurities usually complicate the interpretation. Thus in rocks such as limestone, quartzite, and tonalite, a few dozen micro-metric grains of magnetite may dominate the susceptibility but their orientation–distribution

may not be meaningfully characterized (Borradaile and Stupavsky, 1995). This is exacerbated where k varies in sign between specimens, and for some specimens the AMS is indeterminate because the sign of k varies with direction within the specimen.

The presence of RBMs escalates technical difficulties. Normally, by using a low-field, similar to the geomagnetic field any permanent magnetization is avoided and the $M = kH$ linear response is sufficiently valid. In the Sapphire Instruments SI2B instrument we used, which operates at 19,200 Hz, the peak field is 60 A/m, $\sim 75\%$ of the geomagnetic field in our laboratory). Thus, one may substitute $\mathbf{M} = [k] \cdot \mathbf{H}$ where \mathbf{M} and \mathbf{H} are vectors and $[k]$ is now a second rank tensor describing the anisotropy of susceptibility (AMS). Thus measuring susceptibility (k) in different directions permits the determination of anisotropy of low field susceptibility (AMS) as the tensor $[k]$.

Two conditions may obstruct the linearity of $M(H)$ and thus the determination of AMS. If H is large, say more than 10 times the geomagnetic field $M(H)$ may become non-linear for which the initial hysteresis, convex-upward curve may follow (Jackson et al., 1998):

$$M = kH + \alpha H^2$$

Usually, anisotropy of low-field susceptibility is reproducible. This is valid even for specimens with rather low susceptibility (e.g., $\sim 20 \mu\text{SI}$) if holder corrections and drift corrections are applied carefully. It is also valid for specimens with very high susceptibility, although it may be advisable first to demagnetize them by low temperature demagnetization (Borradaile, 1994; Borradaile et al., 2004). The standard deviation of the drift of the Sapphire Instruments SI2B meter we used is $\sim 0.3 \mu\text{SI}$ over ~ 30 min, although this will depend on the laboratory environment, and may be monitored by a special subroutine in the operating software. In this study, we measured the AMS of a suite of siliceous crystal tuffs, with a macroscopic flow-compaction fabric, with the usual geological goals; to determine the flow axis and thus the provenance of the tuffs. However, for many specimens, the AMS axes and AMS magnitude ellipsoid shape were not reproducible; replicate measurements produced orientations of principal susceptibilities that were different. Some changes occur on a time-scale similar to the duration of a single AMS determination, which requires approximately four minutes when measuring k along seven axes. Our seven-axis measurement scheme has several advantages (Borradaile and Stupavsky, 1995). First, unlike other measurement schemes, four axes of measurement are along body diagonals ($[1\ 1\ 1]$ of crys-

tallography); for these the reference direction of the specimen is equally inclined to the (x, y, z) coordinates of the measurement scheme. The other three measurement axes are parallel to (x, y, z) . The importance of combining body-diagonal and face-parallel measurement axes exists if there is maximum sampling of directional variation. Schemes which use only face-parallel measurements (e.g., Girdler, 1961) fail to do this. The seven-axis scheme has an option to be extended to 15 axes, which permit automatic canceling of holder contributions, but we have found that the increased duration of measurement introduces instrumental drift that may be troublesome in routine studies even with well-behaved material (Borradaile and Stupavsky, 1995). Our measurement program subtracts previously measured holder contributions for the seven-axis scheme.

Uses of low field susceptibility (k_0) and its anisotropy known as AMS, are numerous. Since personal computers became available to control the measuring equipment, hundreds of studies have been published which have used AMS to infer mineral orientation distributions, e.g., in structural geology, petrofabrics, magma-flow, depositional alignment, and environmental geology (Hrouda, 1982; Borradaile and Jackson, 2004; Tarling and Hrouda, 1993; Thompson and Oldfield, 1986). The interpretation of k and especially that of AMS is complex since it depends on the abundances, mineral-susceptibilities, and orientations and spacing of all the different minerals in a specimen, including diamagnetic ones. However, the characteristics of measurement instruments also influence the observations. For example, where RBM are present, Jackson et al. (1998) note that k measurements depend on the inducing field and, if AC fields are used, k may also be frequency-dependent (Jackson and Wörm, 2001). Only where RBM, especially magnetite, hematite and pyrrhotite are absent, may we expect to make reproducible and unique observations of k or AMS since the $M(H)$ response is linear for all fields in paramagnetic and diamagnetic materials. Exposure to high fields may also change “ k_0 ” and AMS where susceptibility is dominated by multidomain accessory RBM (Potter and Stephenson, 1990). It is commonly observed that careful “mineralogically non-destructive” demagnetization may be advisable before reproducible low field susceptibility measurements may be made for specimens rich in multidomain magnetite or pyrrhotite. Low-temperature demagnetization would be the preferable technique since thermal or chemical demagnetization risks mineralogical change and AF demagnetization may reset “ k_0 ” and AMS. In geological applications, tactics must be tailored to suit either paleomagnetic or petrofabric goals and the order in which treatments are applied must be

considered. In this study, we encounter a measurement condition that is fortunately rather rare; AMS results, especially orientations are time-dependent, sensitive to handling, sensitive to replicate measurement and significantly reset by large alternating fields or low-temperature demagnetization.

2. Analysis

Our results are presented as equal-area stereograms showing the individual k_{MAX} , k_{INT} and k_{MIN} axes of specimens as well as the mean axes of a sample of specimens with the confidence region for the mean tensors’ axes, and for the sample (Jelinek, 1978). An important option that Jelinek recommended is the calculation of mean tensors and confidence regions for the measurement at face value, but also where specimen data are normalized to their mean-susceptibility. Comparisons of the two types of mean-orientation for a sample reveal the bias due to high-susceptibility outliers or due to multiple sub-fabric orientations (Borradaile, 2001).

The shape of the AMS magnitude-ellipsoid may be described in terms of its eccentricity or departure from the spherical (isotropic fabric) state and in terms of its symmetry between the extreme prolate and oblate ellipsoids. Structural and some magnetic petrofabric studies retain the original cartographic fabric plot of Flinn (1965) (Fig. 1a) with principal ratios ($a = MAX/INT$) and ($b = INT/MIN$) as axes. This has drawbacks whether it is used for finite strain, magnetic fabric or some measure of orientation distribution. Fabric symmetry or shape, $(a-1)/(b-1)$, is non-linearly dispersed in a circumferential path from one axis to the other (prolate = ∞ ; oblate = 0) and similar eccentricities (i.e., departure from isotropy at the origin) do not plot along a line. Jelinek’s (1978) parameters are superior; the shape parameter T_j is symmetrical (prolate = -1 ; oblate = $+1$) and the eccentricity plots along one axis, with the advantage that it includes a reference to all three principal axes; being logarithmic it also prevents the clustering of data near the origin so typical of weak AMS. However, on cartographic axes low-anisotropy specimens are unnaturally dispersed in the y -axis direction; and the isotropic case plots ambiguously anywhere along the (T_j , $P_j = 1$) axis, Fig. 1b. These minor presentation difficulties are collectively resolved where Jelinek’s parameters are axes of a *polar plot*, in which the isotropic case plots uniquely at the origin, Fig. 1c (Borradaile and Jackson, 2004; Hamilton et al., 2004). Note that some authors economize on calculation, substituting $P = k_{MAX}/k_{MIN}$ for P_j which loses the logarithmic scaling advantage of

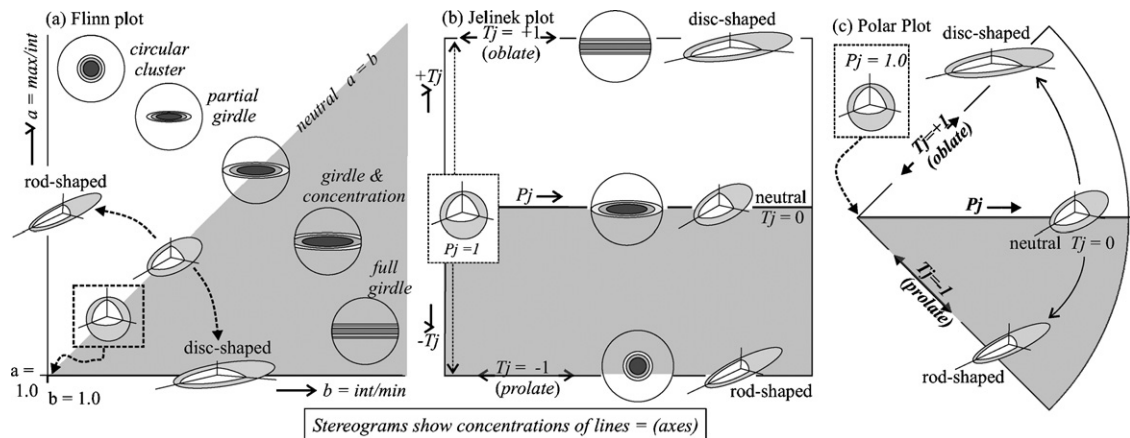


Fig. 1. Where the principal susceptibilities are all of the same sign, the shapes of magnitude ellipsoids representing anisotropy of susceptibility (AMS) may be represented by an ellipsoid. The ellipsoid also qualitatively represents the orientation–distribution of k_{MAX} axes, as shown on stereograms. (a) The Flinn plot was first used, and is still retained in structural geology; however, shape and eccentricity of the ellipsoid are simply associated with a cartographic axis. (b) Jelínek's (1978) parameters for shape (T_j) and eccentricity (P_j) have advantages in that the former is symmetric and the latter is logarithmic with a reference to all three principal axes. Their use on a cartographic plot makes some improvement on the Flinn diagram however, the isotropic case does not plot uniquely and weakly anisotropic states scatter unnaturally along the T_j axis near $P_j = 1$. (c) The last disadvantages disappear if Jelínek's parameters are plotted on a segment of a polar plot (Borradaile and Jackson, 2004).

Jelínek's P_j as well as its reference to the intermediate principal value (Jelínek, 1981).

3. The case study

Our study commenced as a routine magnetic fabric study of some recently discovered felsic pyroclastic flows, in a remote part of northern Ontario, 10 km west of Lake Nipigon and approximately 200 km north of Thunder Bay. The rocks have petrological affinities with granitic–syenitic intrusions approximately 20 km distant, at English Bay on the west shores of Lake Nipigon. The age of the English Bay syenitic–granitic intrusions is 1537^{+10}_{-2} Ma from the U–Pb zircon geochronology of Davis and Sutcliffe (1985). For this tuff Davis obtained an U–Pb age of 1542 ± 3 Ma (Borradaile et al., submitted for publication) confirming the magmatic relationship and the Meso-Proterozoic age of the volcanism. Specimen mean susceptibility (bulk susceptibility) mostly lies between 70 and 250 μSI (Fig. 2f), normally quite adequate for the determination of reproducible susceptibility axial orientations, provided that careful correction is made for the sample holder in each of the orientations in which the specimen is measured and for drift.

However, a routine AMS measurement protocol did not yield reproducible results for most of the sample suite. For example, twelve measurements of a single specimen produce unexpected and unacceptable scatter of principal axes and of fabric-ellipsoid shapes (Fig. 2a and c). Normal investigatory procedures revealed that anisotropy was inconsistent, depending on the dura-

tion of the measurement, the degree of handling in the geomagnetic field of the laboratory, and the degree of relaxation time of the specimen, either in a constant orientation, or inside a magnetic shield (< 2 nT). These clues all point to some time-dependent or viscous magnetic response. Viscous responses cause unstable remanent magnetization (and susceptibility) in both are both very small and large (multidomain = MD) magnetite grains. In magnetite such responses may be troublesome over laboratory time-scales (Dunlop and Özdemir, 1997; p. 262 et seq.) and we shall return to this in conclusion. The concentration of hematite is subordinate to magnetite in these rocks, and since its susceptibility is also $\sim 0.1\%$ that of magnetite, its contribution to this problem is negligible.

Since the noise level of our Sapphire Instruments SI2B coil without a specimen is $\leq 0.2 \mu\text{SI}$ under normal laboratory conditions, AMS instability must be attributable to some specimen interaction with the geomagnetic field (80 A/m) or with the field of the induction-coil measuring susceptibility (60 A/m at 19,200 Hz). The routine instrumental noise test over approximately one hour shows the enormous increase in noise with the specimen in a fixed orientation (Fig. 3a). For specimens with this level of anisotropy and bulk susceptibility the susceptibility difference between successive routine AMS orientations is usually $> 3 \mu\text{SI}$. Clearly, the noise here would blur any true difference in k due to anisotropy, i.e., between successive orientations in the seven-orientation measurement routine. Obviously, measurement procedures of longer duration worsen this

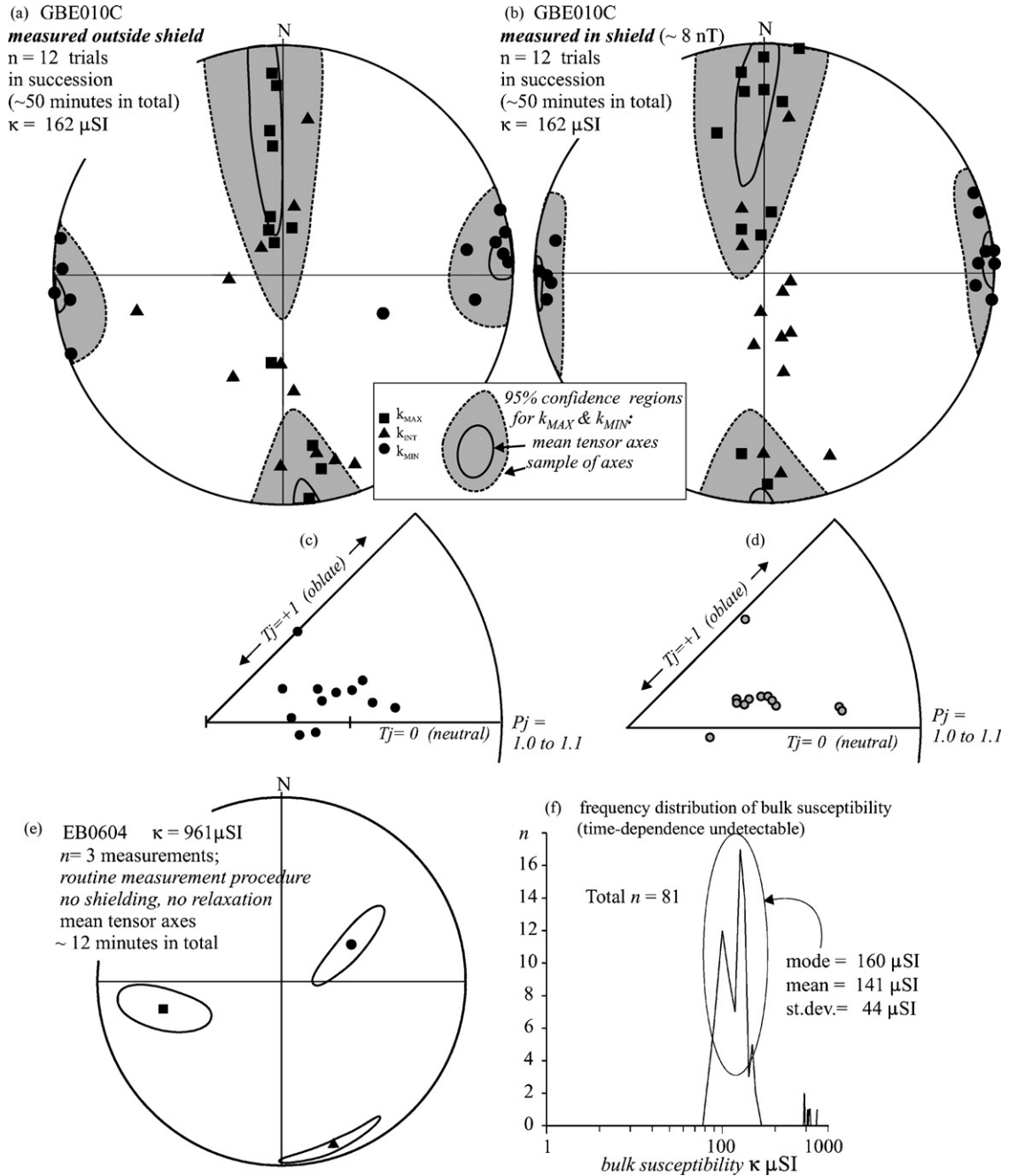


Fig. 2. Time-dependence of AM measurements (all stereograms are equal area). (a) A specimen measured 12 times in succession with no special handling. (b) The same specimen measured 12 times after the specimen had been relaxed for 24 h in a good magnetic shield (<2 nT); axial orientations are more reproducible. The measuring instrument and specimen was also in a magnetic shield during measurement (<10 nT). (c–d) The shapes of the magnitude ellipsoids are also more reproducible when measurements are made inside a shield. (e) Less handling (i.e., fewer measurements) may even produce quite consistent results without a shield; however, the reproducibility is much less than we find in usual AMS studies. (f) Frequency distribution of bulk susceptibility (average of the seven susceptibilities measured in each AMS determination). Bulk susceptibility is not noticeably affected by measurement conditions or their duration.

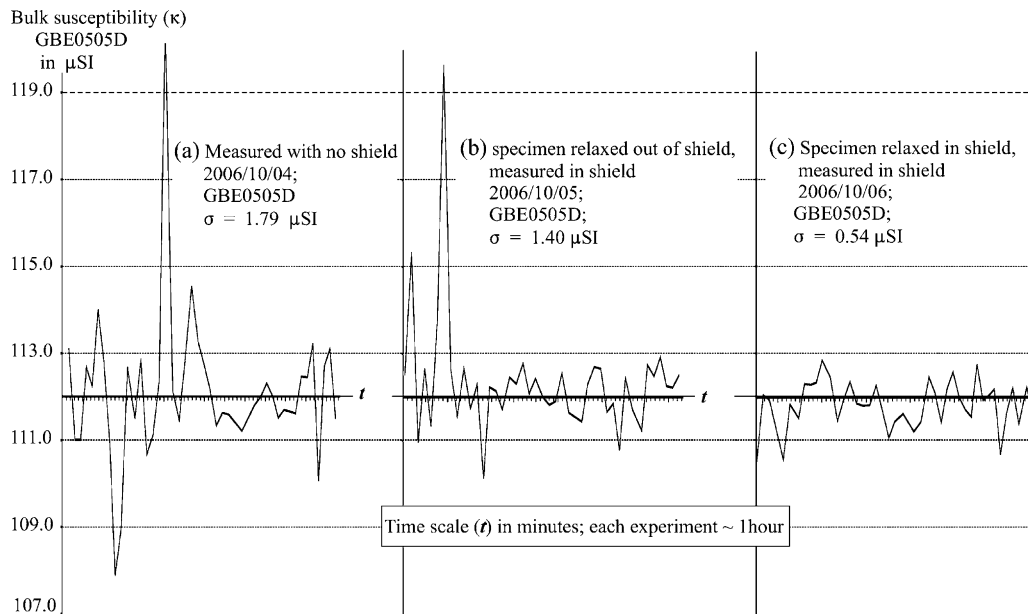


Fig. 3. The routine noise test for the Sapphire Instruments SI2B unit permits comparisons of noise level due to the environment with those due to specimen–environment interaction.

effect; best results were obtained with seven orientations requiring 4–5 min in a separate holder–contribution correction (Borradaile and Stupavsky, 1995).

We shall demonstrate that some improvement is achieved by minimize interaction with natural or artificial fields during and before measurement (cf. Fig. 2b with Fig. 2a). We housed the SI2B instrument inside a large magnetic shield (40 cm × 40 cm × 40 cm shield, ≤ 5nT) which reduced environmental affects on the specimen (Fig. 3a and b). Relaxing the specimen for 24 h in a paleomagnetic-quality shield (≤ 2nT) further improves the subsequent measurement (Fig. 3b and c). Furthermore, the number of replicate measurements quickly encounters the law of diminishing returns; the handling and field-exposure during 12 replicate measurements (each of seven orientations) produces far more scatter than with three replicate measurements (cf. Fig. 2a and e).

4. Rock magnetic properties

For the samples we study, k_{MAX} and k_{INT} are parallel to flow banding. However, the pervasive red hematite pigmentation is clearly secondary; it transgresses the boundaries of xenoliths and flow bands, and it fails to penetrate the interior of some volcanic clasts. Very little hematite is required to pigment a rock and its susceptibility is much less than magnetite. Magnetite, hematite and the most susceptible mafic silicate have k in the ratio

10,000:20:1. Therefore, from the outset it was apparent that AMS was chiefly controlled by magnetite traces, since the abundances of hematite and mafic silicate were at best at accessory concentrations (<1%). Susceptibilities are low but adequate for an AMS study (Fig. 2f).

Multiple mineralogical sources contributing equally to bulk susceptibility commonly present complications in interpretation since their orientation distributions are unlikely to be coaxial (Borradaile and Jackson, 2004). In the absence of a mafic silicate matrix, trace RBMs dominate the interpretation of AMS. Although the anisotropy of RBM may be isolated using the anisotropy of anhysteretic remanences (AARM) technique, in this study the presence of highly coercive hematite prevented the obligatory demagnetization steps. Consequently, the following logical procedures were pursued to evaluate the magnetic mineralogy.

First, IRM acquisition and its decay during progressive AF demagnetization revealed an interesting contrast between specimens with the more stable versus less stable AMS orientations (Fig. 4a and b). The more stable AMS resides in specimens whose remanence cannot be saturated with the maximum DC field available to us (1.0T); although this demagnetizes in alternating fields quite rapidly, it is never completely demagnetized at the highest peak AF available to us (180 mT). Specimens with the least stable AMS nearly saturate their remanence between 60 and 100 mT, indicating the presence of small pseudo-single domain (PSD) and single domain

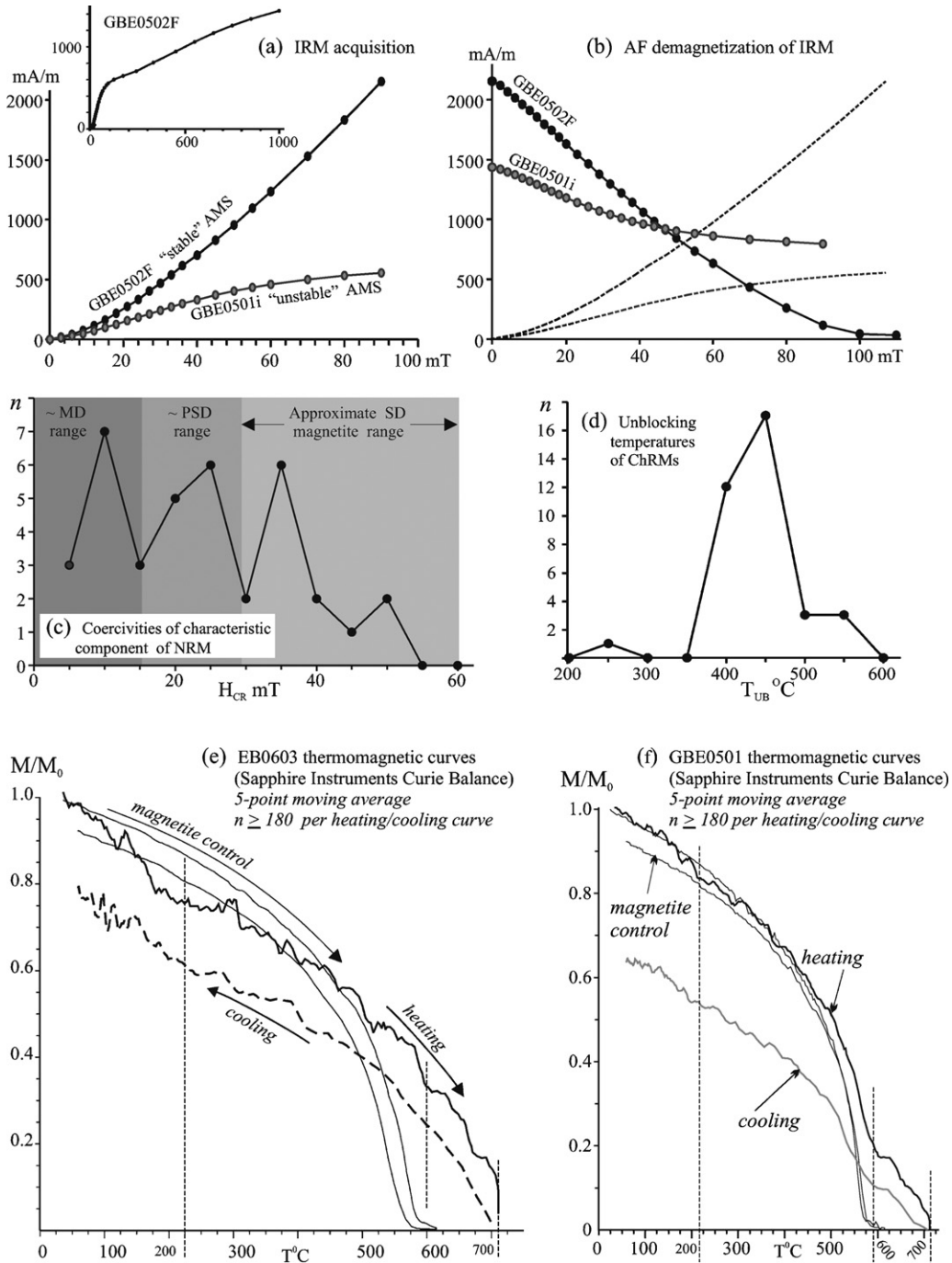


Fig. 4. Simple rock magnetic tests throw some light on the minerals controlling AMS.

(SD) magnetite. However, the presence of hematite in these specimens does prevent their demagnetization.

Second, the resilience to demagnetization of characteristic (arguably primary) components of the natural remanent magnetization may yield clues to the nature of

the RBM. Incremental demagnetization of 37 specimens (after all susceptibility studies were made) revealed that significant NRM components reside in coercivity ranges equivalent to MD, PSD and SD magnetite (Fig. 4c). Unblocking temperatures from thermal demagnetiza-

tion of another set of 37 specimens shows that most unblocking temperatures occur just below 500 °C, and none above 600 °C. The most common unblocking temperatures of ChRMs commonly occur just below the Curie temperature of the host mineral. This information is equivocal since the Curie temperatures of magnetite and hematite are ~580 and ~700 °C, respectively.

Thirdly, thermomagnetic tests using a Sapphire Instruments (SI6) Curie balance reveal the decay of saturation remanence with temperature. Curie- or Néel temperatures are shown for specimens with more stable (Fig. 4e) and less stable (Fig. 4f) AMS orientations. A typical specimen with stable AMS shows the dominance of hematite with slight inflection points that suggest the

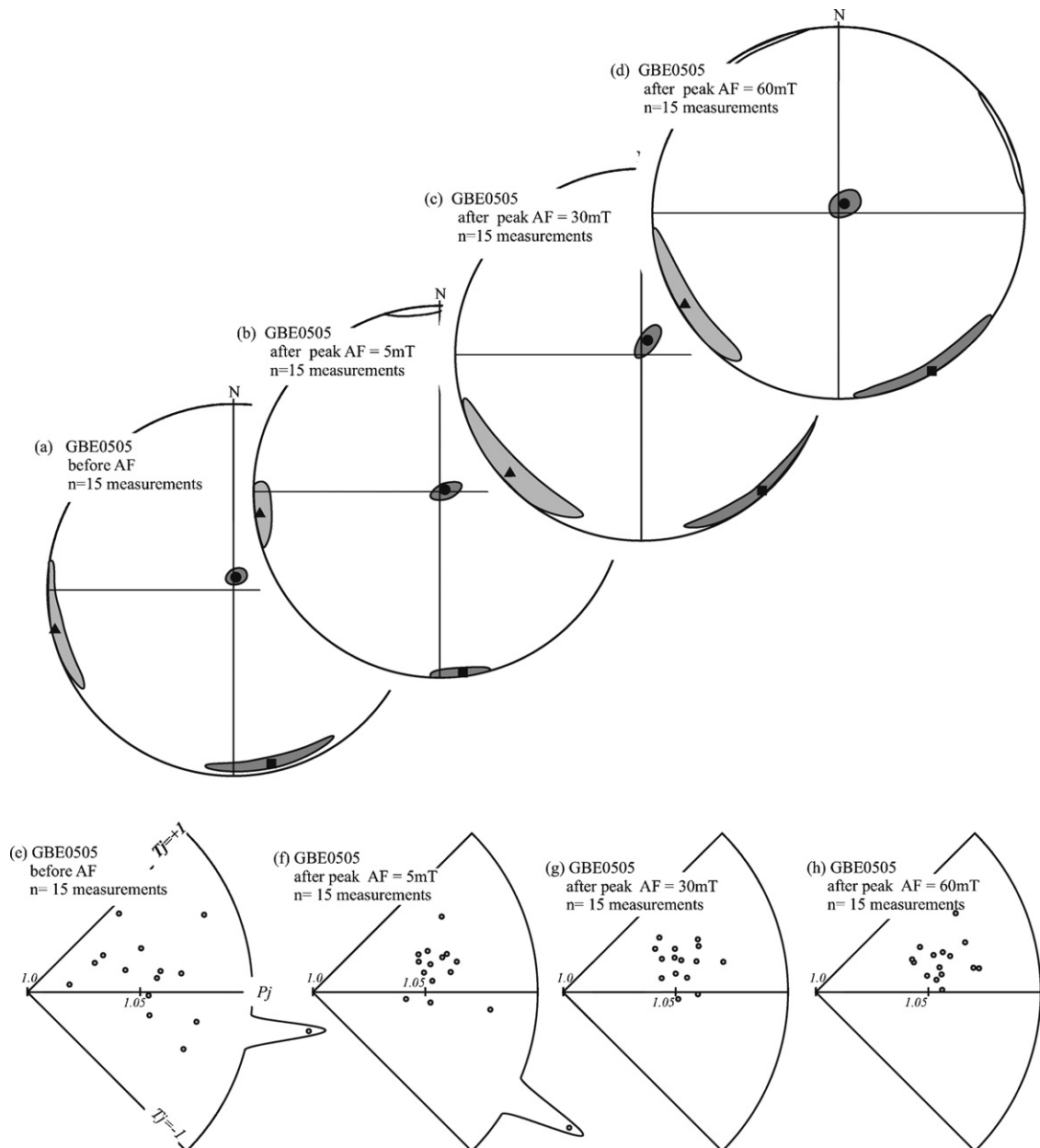


Fig. 5. Fifteen replicate measurements on the same specimen before and after certain steps of incremental AF demagnetization. (a–d) The orientation of the mean tensor changes significantly after AF demagnetization to 30 mT, and during AF demagnetization the planar component of the AMS fabric is enhanced, as shown by the shapes of the confidence regions for the axes of the mean tensor. (e–h) The shapes of the AMS magnitude ellipsoid are more reproducible as AF demagnetization progresses.

presence of minerals with Curie or Neel temperatures of $\sim 210^\circ\text{C}$ (? titanomagnetite or titanohematite) and at 700°C (hematite); there is a dubious indication of an inflexion point associated with magnetite (580°C). A specimen with a less stable AMS shows a dominant Curie temperature due to magnetite ($\sim 580^\circ\text{C}$); with a subsidiary critical temperature at $\sim 700^\circ\text{C}$ (hematite); the inflexion at 210°C may also be present (Fig. 4f).

5. Effects of AF and low-temperature demagnetization on AMS-stability

Potter and Stephenson (1990) showed us clearly that exposure to high fields, including the alternating fields used in AF demagnetization changed bulk susceptibility (k) slightly, usually the changes are $\sim 0.1\%$. However, since AMS is defined by small differences ($\sim 1\%$) in k

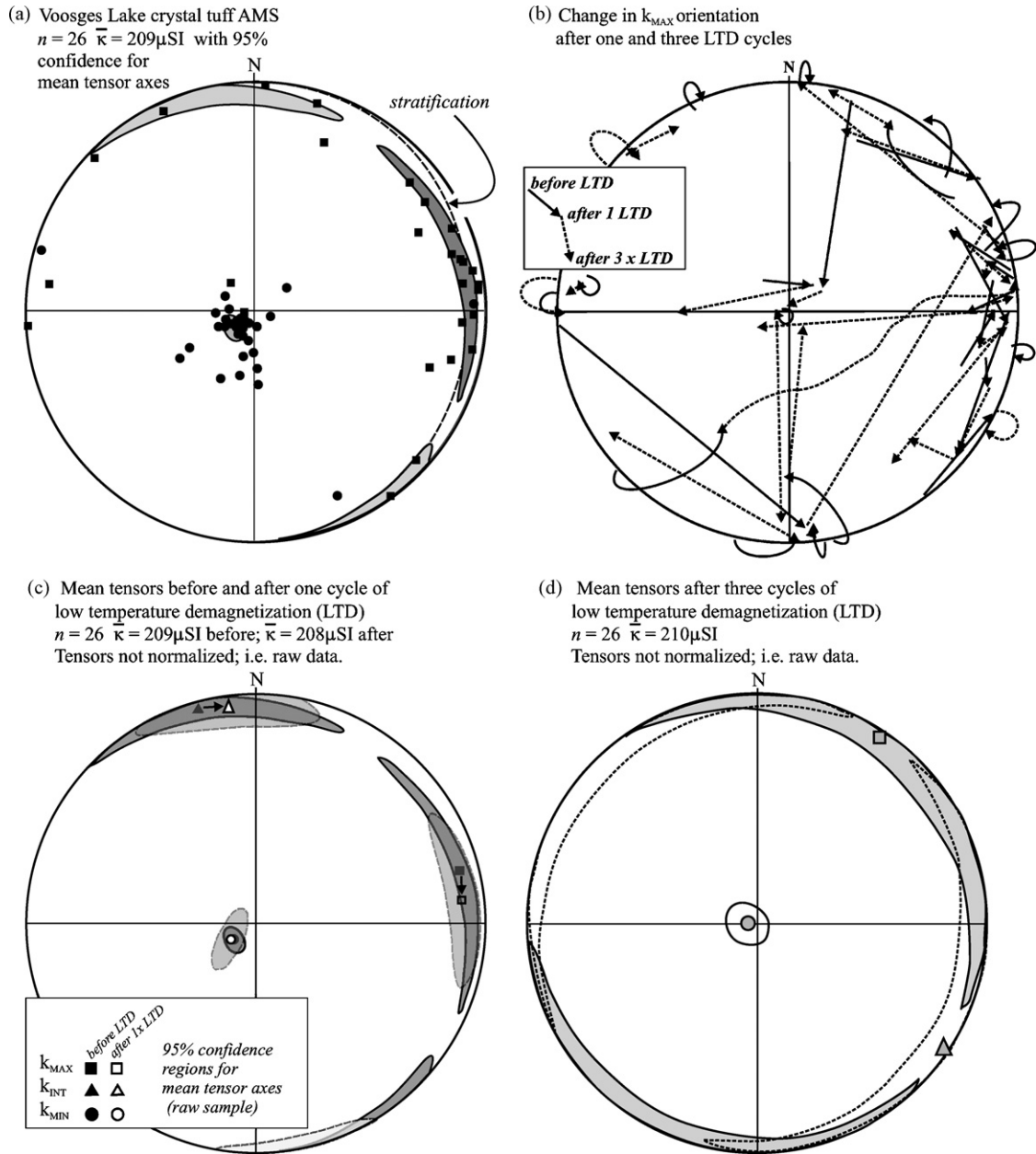


Fig. 6. (a) Measurement of a suite of the specimens with no special shielding or special handling. (b) Erratic changes in their AMS axes after one cycle of low temperature demagnetization (LTD to 77 K). (c–d) Mean tensor axes for the suite, with their confidence cones after one and after three LTD cycles. Note the enhanced definition of a planar fabric but the change in directions of the mean k_{MAX} and mean k_{INT} .

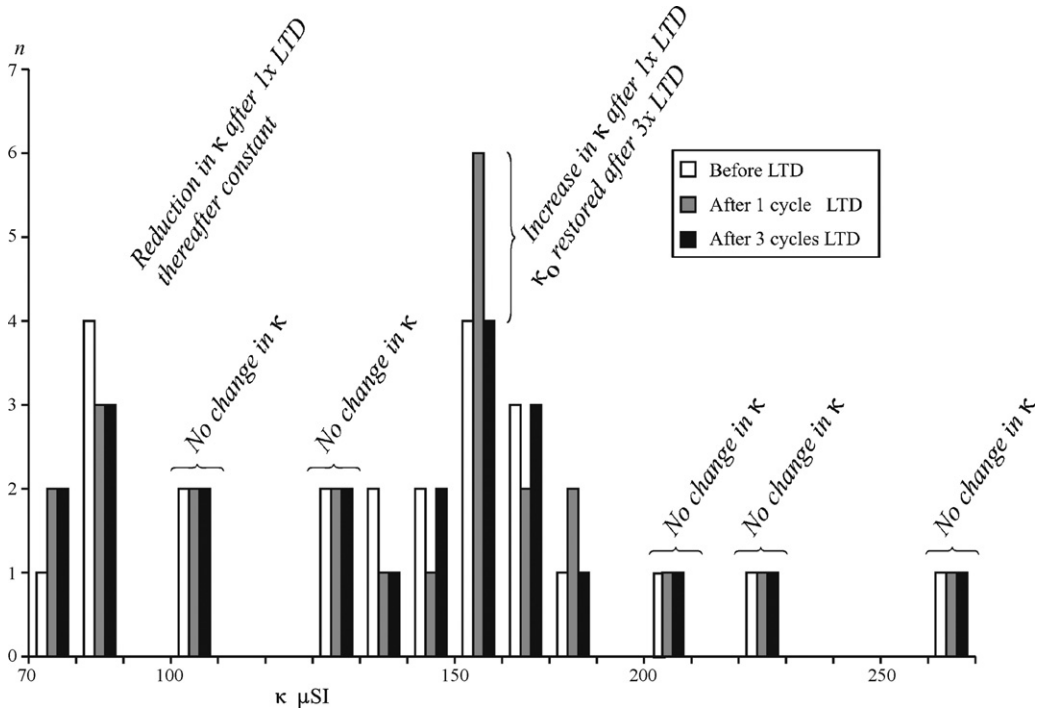
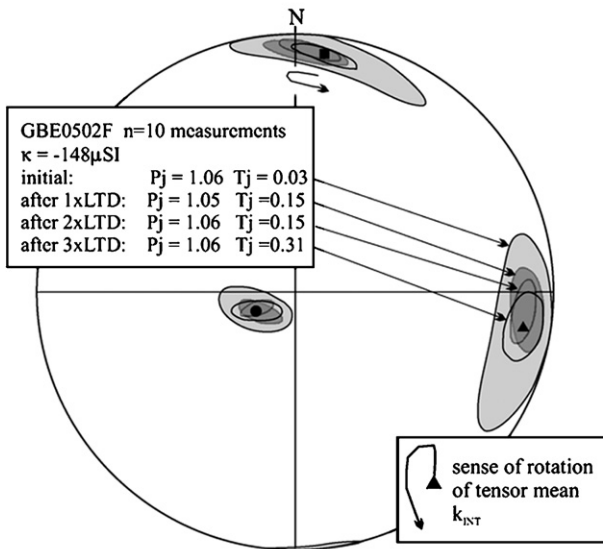


Fig. 7. Inconsistent changes in bulk susceptibility for different specimens with one and three cycles of LTD.

(a) GBE0502F $n = 10$ measurements
orientations stable before and after LTD



(b) GBE0502F $n = 10$ measurements
fabrics most stable after 1x LTD

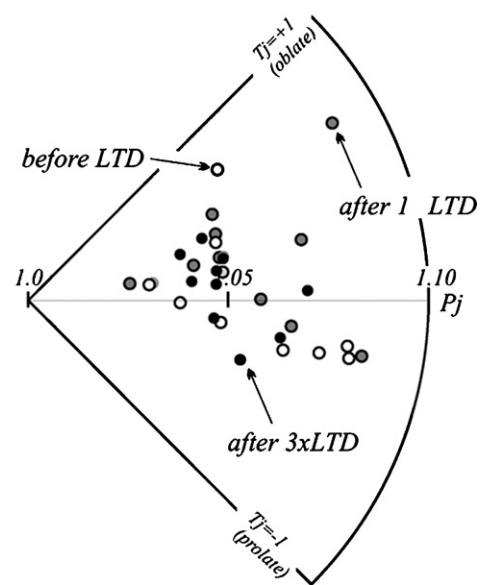


Fig. 8. Ten replicate measurements of a specimen with “stable AMS”, before and after cycles of LTD. (a) Mean tensor has reproducible axial orientations but a gradual improvement of concentration of specimen axes, shown by the progressively smaller confidence regions for the mean axes. (b) AMS magnitude ellipsoid shapes are more reproducible after LTD.

along different axes, it is clear that any small high-field change in k is much more apparent in changes of the AMS axes. In multidomain magnetite, AMS is determined by the grain-shape and the internal arrangement of domain-walls. Potter and Stephenson demonstrated that high fields (>10 mT) sufficed to cause essentially permanent re-arrangements of domain walls with slight

changes in k which explains the more noticeable changes in AMS axial orientations.

A specimen with relatively stable AMS orientations was measured 15 times in rapid succession, without any shielding, or special handling. The routine measurement procedure produced results with moderate scatter, as shown by the 95% confidence regions for the mean

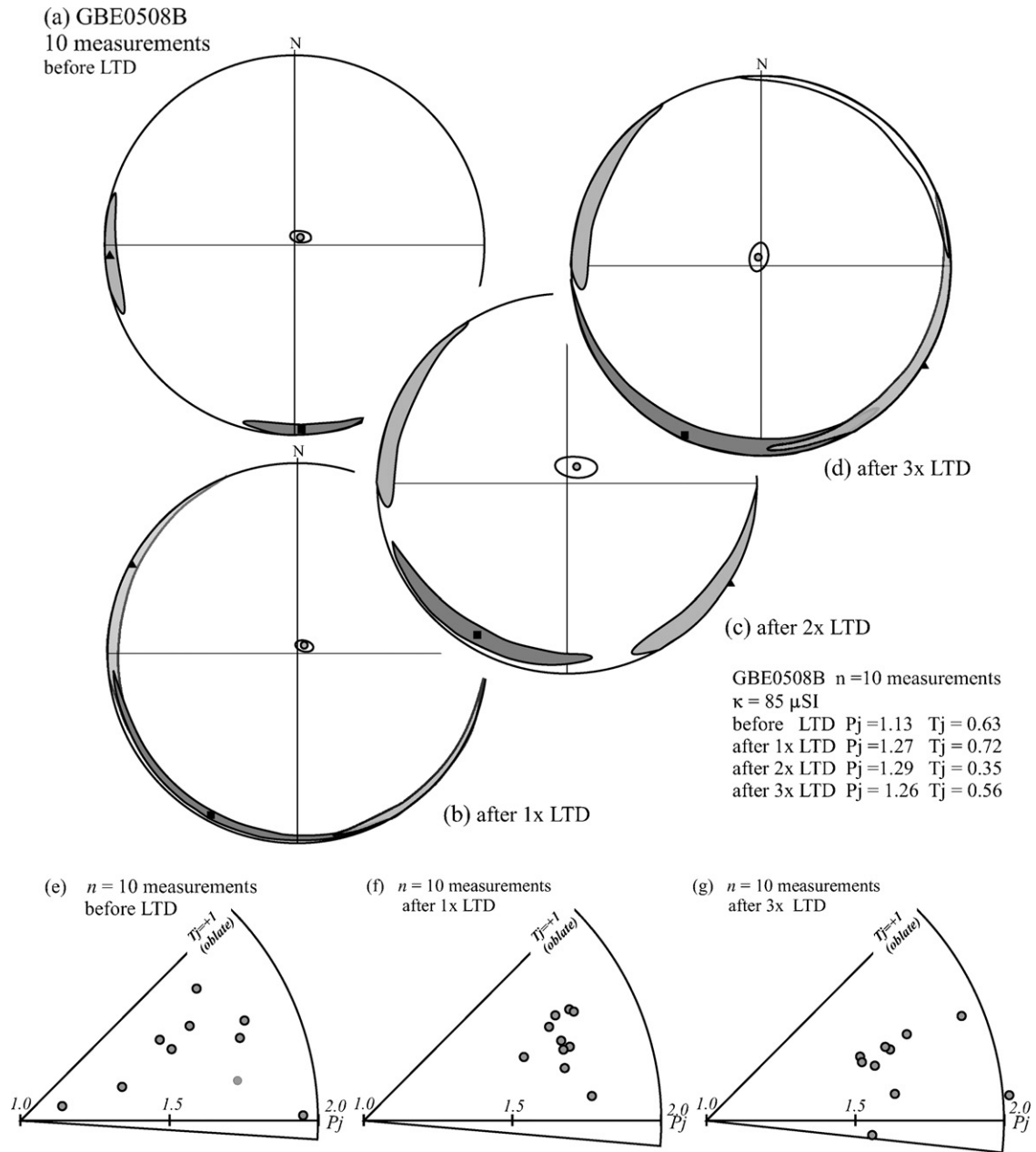


Fig. 9. Ten replicate measurements of a specimen with fairly stable AMS. (a–d) Orientations of mean axes change slightly after one TD cycle but are thereafter stable. However, the dispersion of specimen axes emphasizes a more planar fabric as LTD cycles are increased. (e–f) AMS magnitude ellipsoid shapes appear most reproducible after one LTD cycle.

tensor (Fig. 5a) but with poorly defined shapes for the magnitude ellipsoid (Fig. 5e). Further sets of 15 rapid measurements after demagnetization to peak AF fields of 5, 30 and 60 mT change the AMS axial orientations significantly, improving the definition of the planar

component of the magnetic fabric shown by the elongate coplanar confidence regions for the mean k_{MAX} and k_{INT} . Progressive AF demagnetization also reduces the scatter in ellipsoid shapes (Fig. 5f–h). AF demagnetization steps should have re-arranged domain walls

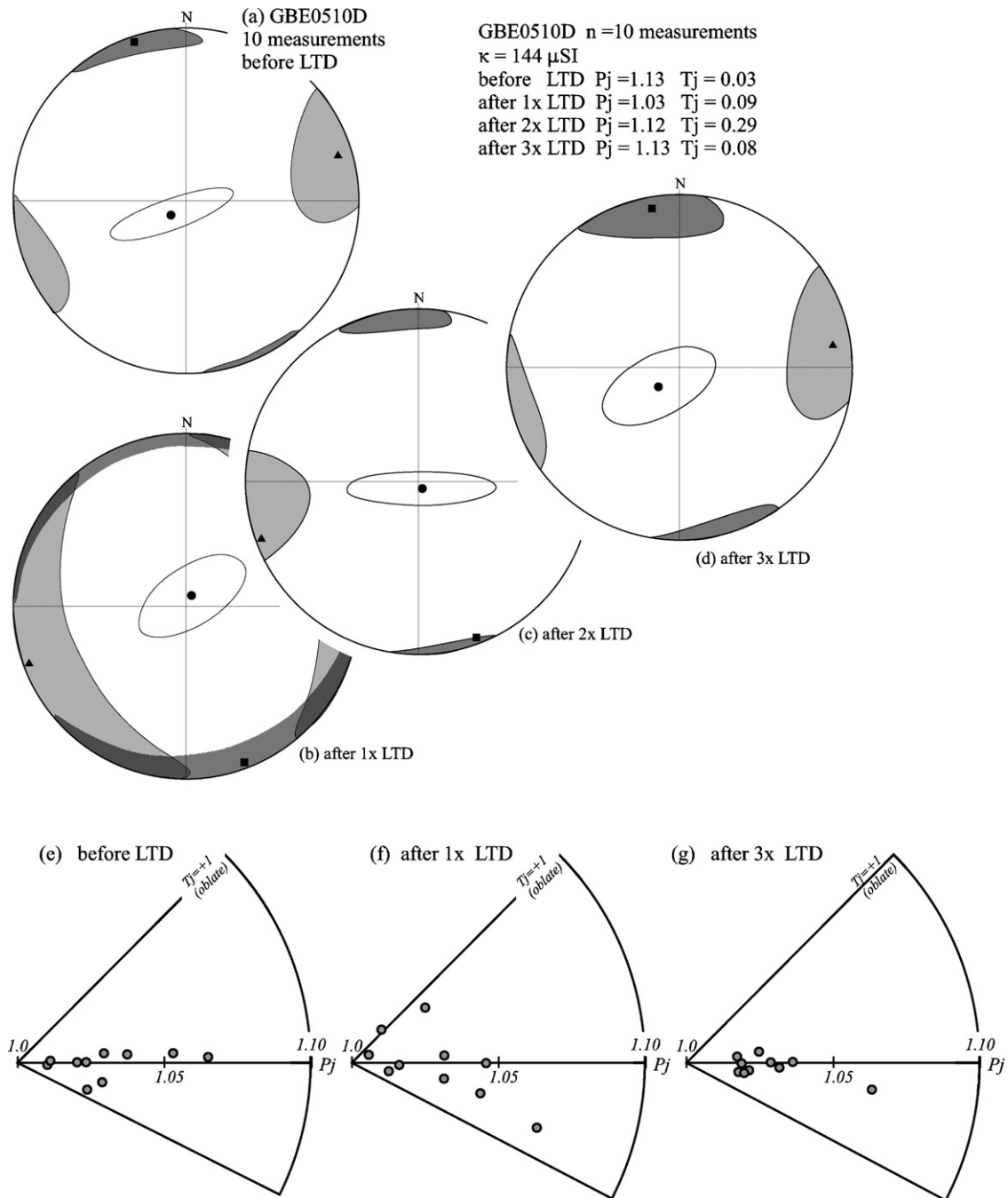


Fig. 10. Ten replicate measurements of a specimen with a fairly unstable AMS. (a–d) The mean axis of the sample of measurements for this specimen change orientation significantly as cycles of LTD are applied. Reproducibility may be improved after three cycles of LTD but this is debatable. (e–g) Shape of the magnitude ellipsoid may become more reproducible after three cycles of LTD.

associated with MD and PSD magnetite in progression so that the most stable results presumably correspond to MD magnetite grain-shapes, without contributions from meta-stable domain walls. Of course, SD magnetite has k_{MIN} parallel to its long axis and k_{MAX} parallel to its shortest dimension (Jackson, 1991; Potter and Stephenson, 1988), giving rise to rare but readily identified inverse fabrics and more obfusc-blended fabrics where SD magnetite subfabrics compete with other kinematically intuitive (“normal”) subfabrics (Rochette et al., 1992; Ferré, 2002). A few specimens in the suite do show either inverse SD fabrics (vertical k_{MAX} axes, Fig. 11) or in some cases blended SD–MD fabrics. It is sometimes difficult to distinguish the latter from what may be real exceptions to the average flow direction.

LTD also rearranges magnetite domain when it is cooled through its Verwey transition (~120 K) by immersion in liquid Nitrogen (77 K) and then allowed to warm to room temperature. Performed inside a magnetic shield, this procedure assures that the maximum effects of grain-shape are revealed for magnetite and, for paleomagnetists, that spurious domain-wall remanence is erased. Three LTD cycles usually optimize demagnetization, and never more than five (Borradaile, 1994; Borradaile et al., 2004; Middleton et al., 2004). Our initial attempt to stabilize AMS directions for a sample of 26 specimens, each measured just once (Fig. 6a), did tighten confidence regions around the mean tensor axes (Fig. 6c) with one LTD cycle but this improvement was lost when a second and third LTD cycle were applied (Fig. 6d). Erratic changes in the axial orientations of

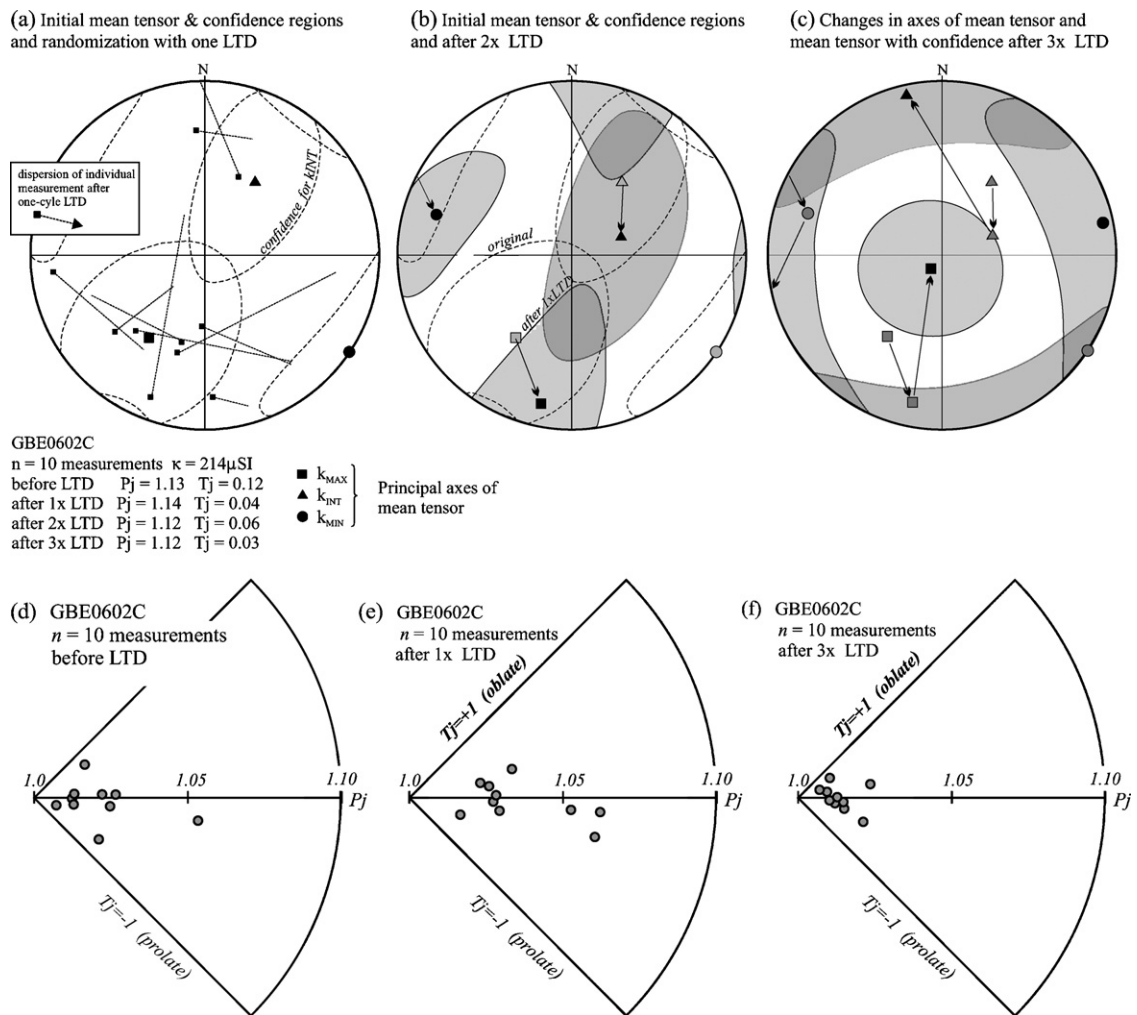
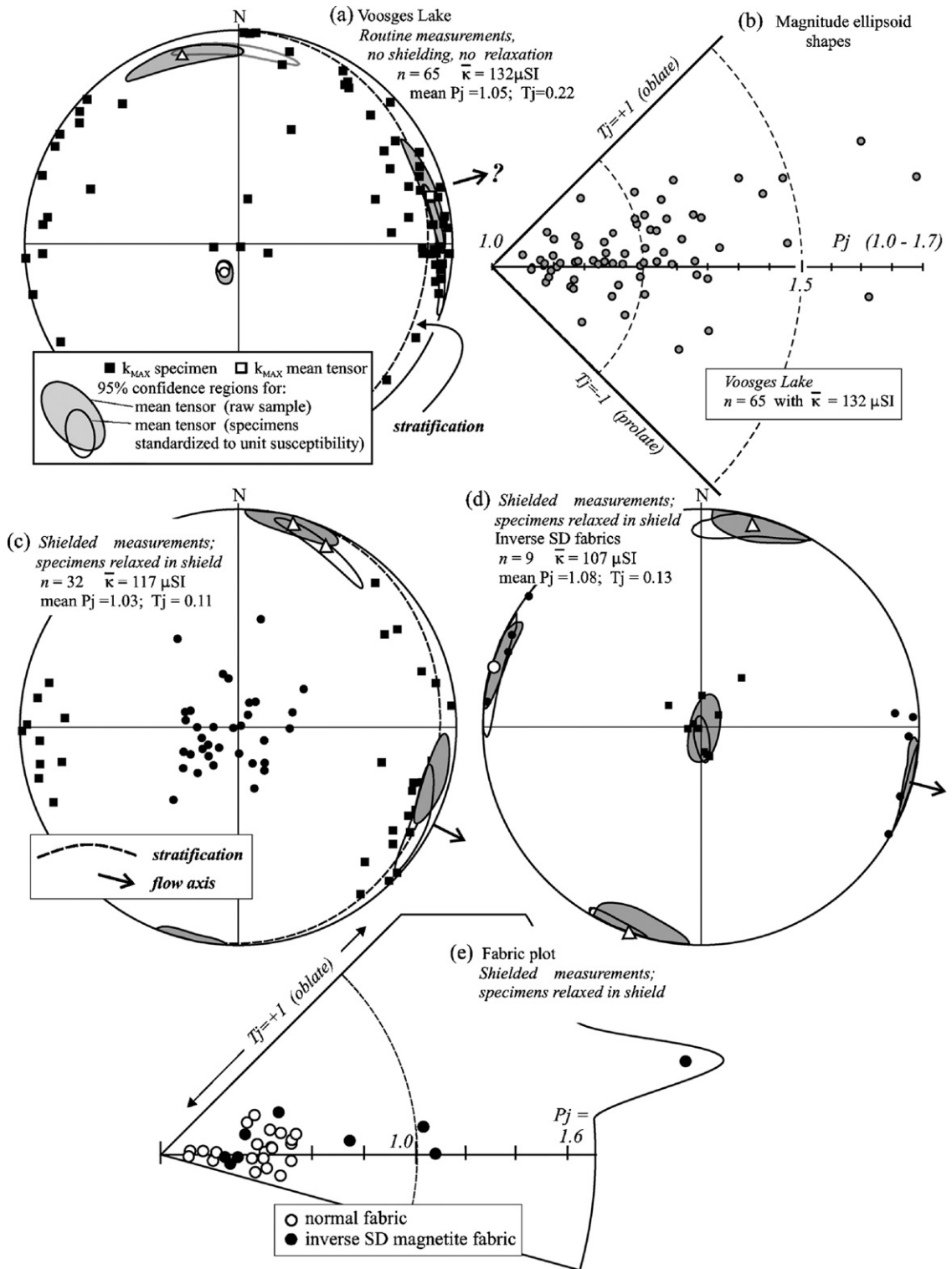


Fig. 11. Replicate measurements of the least stable type of specimen before and after LTD cycles. (a–c) Erratic changes in the mean axis and confidence regions unacceptably large. (d–f) Shapes of magnitude ellipsoids do however seem more reproducible after three LTD cycles.



individual specimens are seen in Fig. 6b. Fig. 7 shows the somewhat chaotic changes in k_0 after one and three LTD cycles; the behaviour is not systematic although the stereogram of Fig. 6c suggests that a single LTD cycle optimizes the stabilization of AMS axes.

A more satisfactory specimen reveals rather stable AMS axial orientation when measured 10 times before and after LTD cycles (Fig. 8a). The axes confidence regions are smallest after one LTD cycle, but thereafter enlarge, although the orientation of the mean axes changes imperceptibly. The AMS magnitude ellipsoid shape is also best defined after one LTD cycle (Fig. 8b).

Less stable specimens are illustrated in Figs. 9 and 10. LTD causes significant changes in AMS axial orientations, even swapping of principal axes, and changes in ellipsoid shape that may be best defined after one (Fig. 9f) or after three (Fig. 10g) LTD cycles. In the worst specimen, 10 replicate measurements fail to define satisfactory mean axial orientations (Fig. 11a–c), although three LTD cycles slightly improved the definition of orientation (Fig. 11c) and shape (Fig. 11f).

6. Conclusions and best measurement procedure

Some of the time-dependent susceptibility variation observed is attributable to geomagnetic field effects in the laboratory, since relaxing the specimens in a shield improves the reproducibility of axial orientations. However, the AC measurement procedure using a peak field that is $\sim 60\%$ of the geomagnetic field also produces some effect since the larger the number of replicate measurements, the less reproducible are the orientations of AMS axes (cf. Fig. 2b with 3 measurements with Fig. 2a, 12 measurements). Our choice of a seven-axis measurement scheme, in use since 1995, provides a better sampling of orientation possibilities during AMS measurements than the traditional 6 and 12 orientation schemes. Since that procedure is better for rocks with reproducible, easily measurable AMS, it cannot be the source of directional instability here as suspected by a reviewer. Dunlop and Özdemir (1997, p. 262 et seq.) note that the viscous magnetization of magnetite, conveniently considered as a viscosity coefficient ($S = dM/dt$) may peak for small SD grains ($\sim 0.03 \mu\text{m}$) and then again for PSD grains in the size range 5–10 μm . Coer-

civities suggest both these grain sizes appear to be present (Fig. 4) and in a few specimens the presence of an inverse AMS fabric indicates domination by SD behaviour (Fig. 11b). The matter is complicated since the viscosity coefficient is expected to be different for acquisition and decay, and to be affected by the initial state and stability of magnetization. S_{DECAY} is expected to be less than $S_{\text{ACQUISITION}}$ (Dunlop and Özdemir, 1997) which is unfortunate for AMS research in rocks such as those studied here.

Clearly, measurement conditions cannot always be ignored in the study of low-field magnetic anisotropy. Numerous workers have recognized aspects of the problem involving field-dependence, frequency dependence and viscous effects (Borradaile et al., 1992; Jackson et al., 1998; Jackson and Wörm, 2001; Mullins and Tite, 1973; Potter and Stephenson, 1990; de Wall, 2000; de Wall and Wörm, 1993). However, those studies usually involved extreme measurement conditions or specially selected materials. The specimens we examined present a more subtle case which is hopefully rare but which could be overlooked without replicate measurements.

Low temperature and AF demagnetization may improve the definition of AMS axial orientations in some specimens. However, the improvements are not consistent enough to justify their use as aids to routine AMS measurement and the required degree of demagnetization is not predictable. Indeed, it is clear for some specimens that any handling may change the AMS, including the AC induction coil measurement itself. We believe the best procedure is to first measure a suite of specimens using the routine procedure; without special handling or shielding. For us, such results indicate considerable scatter of axial orientations (Fig. 12a) and a very broad spread of ellipsoid shapes (Fig. 12b). The same specimens should then be relaxed inside a good magnetic shield, in our case at $< 2 \text{ nT}$ for at least 24 h. A single measurement of each specimen is then performed with the measuring instrument inside a large magnetically shielded space, in our case with a residual field $< 10 \text{ nT}$. The shielding should be several coil-lengths distance from the measurement coil (Dr. M. Stupavsky, pers. comm.). Colleagues measuring magnetic susceptibility in tills also have benefited from the use of shielding around the measuring apparatus (Gravenor et al., 1973;

Fig. 12. (a) Routine AMS specimens without shielding or special handling yield unreproducible results. One campaign of measurement here suggests a mean flow axis ENE-WSW. (b) Corresponding AMS magnitude ellipsoid shapes are rather widely scattered. (c) When the same specimens are relaxed for 24 h in a good magnetic shield ($< 2 \text{ nT}$) and then measured with the Sapphire Instruments SI2B inside a magnetic shield ($< 10 \text{ nT}$) reproducible AMS axes indicate a ESE-WNW flow axis in the foliation, which is also parallel to the field stratification. (d) A subset of these specimens shows inverse fabrics that are nevertheless kinematically compatible with the flow axis shown in (c). (e) AMS magnitude ellipsoids are well defined using this improved measurement procedure and generally less anisotropic (lower P_j), with the exception of inverse fabrics (SD magnetite).

Stupavsky et al., 1974). With shielding, our axial orientations are much better concentrated (Fig. 12c and d) and the dispersion of magnitude-ellipsoid shapes is reduced (Fig. 12e). The normal AMS axial fabrics define a flow axis $\sim 110^\circ$ or 290° within the flow plane which is recognizable in the field and parallel to the girdle of k_{MAX} and k_{INT} axes (Fig. 12c). The much smaller sample of specimens with inverse SD fabrics may be interpreted with similar flow axes (Fig. 12d).

The rarity of time-dependent AMS leaves us unconcerned but a simple test for its presence is to relax the specimens and perhaps also measure them in a shielded environment and then repeat the measurement some hours later. It is doubtful that measurements would be improved using methods other than the rapid AC induction coil method. For example, the torsion magnetometer requires longer measurement times and whereas the applied field is static, it is also large (Jelínek, 1985).

Acknowledgments

This work was supported by NSERC equipment and operating grants to G. Borradaile. Catherine Borradaile helped with sampling and field logistics and Bob Middleton (East West Resources, Vancouver and Thunder Bay) introduced us to this problem. Mike Stupavsky (Sapphire Instruments, sapphiresmagnetics.com) advised us concerning equipment conditions and magnetic shielding.

References

- Borradaile, G.J., 1994. Low-temperature demagnetization and ice-pressure demagnetization in magnetite and hematite. *Geophys. J. Int.* 116, 571–584.
- Borradaile, G.J., 2001. Magnetic fabrics and petrofabrics: their orientation distributions and anisotropies. *J. Struct. Geol.* 23, 1581–1596.
- Borradaile, G.J., Jackson, M., 2004. Anisotropy of magnetic susceptibility (AMS): magnetic petrofabrics of deformed rocks. In: Martin-Hernandez, F., Lünenburg, C.M., Aubourg, C., Jackson, M. (Eds.), *Magnetic Fabric: Methods and Applications*, 238. Geological Society London, London, pp. 299–360 (special publication).
- Borradaile, G.J., Stupavsky, M., 1995. Anisotropy of magnetic susceptibility: Measurement schemes. *Geophys. Res. Lett.* 22, 1957–1960.
- Borradaile, G.J., Davis, D.W., Middleton, R.S., Geneviciene, I. Late Proterozoic remagnetization of Mid-Proterozoic rocks, Nipigon Graben of Northern Ontario, submitted for publication.
- Borradaile, G.J., Lucas, K., Middleton, R.S., 2004. Low-temperature demagnetization isolates stable vector components in magnetite-bearing diabase. *Geophys. J. Int.* 157, 526–536.
- Borradaile, G.J., Puumala, M., Stupavsky, M., 1992. Anisotropy of complex magnetic susceptibility (ACMS) as an indicator of strain and petrofabric in rocks bearing sulphides. *Tectonophysics* 202, 309–318.
- Davis, D.W., Sutcliffe, R.H., 1985. U–Pb ages from the Nipigon “Plate” (sic) and northern Lake Superior. *Geol. Soc. Am. Bull.* 96, 1572–1579.
- de Wall, H., Wörm, H.-U., 1993. Field dependence of magnetic anisotropy in pyrrhotite: effects of texture and grain shape. *Phys. Earth Planet. Interiors* 76, 137–149.
- de Wall, H., 2000. The field-dependence of AC susceptibility in titanomagnetites: implications for the anisotropy of magnetic susceptibility. *Geophys. Res. Lett.* 27, 2409–2411.
- Dunlop, D.J., Özdemir, Ö., 1997. rock magnetism: fundamentals and frontiers. In: *Cambridge Studies in Magnetism*. Cambridge University Press, 573 pp.
- Ferré, E.C., 2002. Theoretical models of intermediate and inverse AMS fabrics. *Geophys. Res. Lett.* 29 (7), p. 31-1-4.
- Flinn, D., 1965. On the symmetry principle and the deformation ellipsoid. *Geol. Mag.* 102, 36–45.
- Girdler, R.W., 1961. The measurement and computation of anisotropy of magnetic susceptibility in rocks. *Geophys. J. R. Astronom. Soc.* 5, 34–44.
- Graham, J.W., 1954. Magnetic susceptibility anisotropy, an unexploited petrofabric element. *Geol. Soc. Am. Bull.* 65, 1257–1258.
- Gravenor, C.P., Stupavsky, M., Symons, D.T.A., 1973. Paleomagnetism and its relation to till deposition. *Can. J. Earth Sci.* 10, 1068–1078.
- Hamilton, T.D., Borradaile, G.J., Lagroix, F., 2004. Sub-fabric identification by standardization of AMS: an example of inferred neotectonic structures from Cyprus. In: Martin-Hernandez, F., Lünenburg, C.M., Aubourg, C., Jackson, M. (Eds.), *Magnetic Fabric: Methods and Applications*, 238. Geological Society London, London, pp. 527–540 (special publication).
- Hrouda, F., 1982. Magnetic anisotropy of rocks and its application in geology and geophysics. *Geophys. Surv.* 5, 37–82.
- Ising, G., 1942a. On the magnetic properties of varved clay. *Arkiv för Matematik, Astronomi och Fysik* 29A, 1–37.
- Ising, G., 1942b. Den varviga lerans magnetiska egenskaper. *Geologiska Föreningen i Stockholm Förhandlingar* 64, 126–142.
- Jackson, M., Moskowitz, B., Rosenbaum, J., Kissel, C., 1998. Field-dependence of AC susceptibility in titanomagnetites. *Earth Planet. Sci. Lett.* 157, 129–139.
- Jackson, M., 1991. Anisotropy of Magnetic Remanence: a brief review of mineralogical sources, physical origins, and geological application, and comparison with susceptibility anisotropy. *Pure Appl. Geophys.* 136, 1–28.
- Jackson, M.J., Wörm, H.-U., 2001. Anomalous unblocking temperatures, viscosity and frequency-dependent susceptibility in the chemically-remagnetized Trenton Limestone. *Phys. Earth Planet. Interiors* 126, 27–42.
- Jelínek, V., 1978. Statistical processing of anisotropy of magnetic susceptibility measures on group of specimens. *Stud. Geophys. Geodet.* 22, 50–62.
- Jelínek, V., 1981. Characterization of the magnetic fabrics of rocks. *Tectonophysics* 79, T63–T67.
- Jelínek, V., 1985. The physical principles of measuring magnetic anisotropy with the torque magnetometer. *Travaux Geophysiques* 33, 177–198.
- Middleton, R.S., Borradaile, G.J., Baker, D., Lucas, K., 2004. Proterozoic diabase sills of northern Ontario: magnetic properties and history. *J. Geophys.* 109, B02103, doi:10.1029/2003JB002581.
- Mullins, C.E., Tite, M.S., 1973. Magnetic viscosity, quadrature susceptibility, and frequency dependence of susceptibility in single-domain assemblies of magnetite and maghemite. *J. Geophys. Res.* 78, 804–809.

- Potter, D.K., Stephenson, A., 1988. Single-domain particles in rocks and magnetic fabric analysis. *Geophys. Res. Lett.* 15, 1097–1100.
- Potter, D.K., Stephenson, A., 1990. Field-impressed anisotropies of magnetic susceptibility and remanence in minerals. *J. Geophys. Res. B Solid Earth* 95, 15573–15588.
- Rochette, P., Jackson, M., Aubourg, C., 1992. Rock magnetism and the interpretation of anisotropy of magnetic susceptibility. *Rev. Geophys.* 30, 209–226.
- Stupavsky, M., Symons, D.T.A., Gravenor, C.P., 1974. Paleomagnetism of the Port Stanley Till, Ontario. *Geol. Soc. Am. Bull.* 85, 141–144.
- Tarling, D.H., Hrouda, F., 1993. *The Magnetic Anisotropy of Rocks*. Chapman & Hall, London, 217 pp.
- Thompson, R., Oldfield, F., 1986. *Environmental Magnetism*. Allen & Unwin, London, 227 pp.